AIAA JOURNAL
Vol. 44, No. 8, August 2006

Laboratory Investigation of Detrainment in Vortex Wakes

H.-T. Liu*
StereoVision Engineering, Bellevue, Washington 98006

Detrainment in vortex wakes is a delicate phenomenon that has been predicted to occur only at high Froude numbers in stratified fluids, as a result of imbalance of buoyancy between fluids inside and outside the vortex wakes. Such a phenomenon rarely manifests in full-scale flights because the required high-Froude-number conditions are seldom met. Physical modeling of the phenomenon using small-scale wings must be conducted in a fluid with a very weak stratification, which is difficult to prepare and maintain in the laboratory. Furthermore, the detrainment flow is so weak that its observation relies on the generation of very clean vortex wakes. Consequently, only limited laboratory results are available and the phenomenon is by no means well understood. Detrainment in vortex wakes has not been observed directly but inferred from their kinematics, that is, acceleration and deceleration. The first ever visual evidence of the detrainment phenomenon is provided. The stringent requirements were met by 1) conducting towing-tank experiments using a two-dimensional vortex generator and a clean wing model suspended on fine wires and 2) preparing weakly stratified fluids using brine and/or heat. Based on visual results, effects of detrainment on the vortex wakes were studied qualitatively and quantitatively.

I. Introduction

WITH the advent of large aircraft, the capability to determine wake vortex intensities accurately has become very important. Because light aircraft passing through strong wakes may have trouble in maintaining control, aircraft spacing at congested airports is dictated by the characteristics of vortex wakes left behind by larger aircraft. Once generated, vortex wakes are affected by various atmospheric phenomena such as stratification, wind shear, and turbulence. An in-depth understanding of the effects of such phenomena on the evolution of vortex wakes is important to predict their strength and whereabouts. In particular, understanding mechanisms that bring about wake dissipation would provide information to enable augmentation of the decay process, which would help accelerate destruction of wake vortices and ease airport congestion.

Early studies have demonstrated that atmospheric conditions have a strong influence on the evolution of aircraft vortices.[1−3] There is inadequate information from full-scale flight tests or laboratory investigations because of difficulties in controlling test conditions and in collecting quantitative results from test results. Although empirical, analytical, and numerical models have been developed to investigate the vortex wake phenomenon, they have not been subject to thorough verification due to the lack of quantitative field or laboratory data.[2−6]

Towing-tank experiments were conducted to simulate turbulence and ground effects on vortex wakes.[7,8] Laboratory results have shown that turbulence with dominant scales comparable to the vortex separation tends to promote sinusoidal or linking instability. The measured lifespan agrees reasonably well with theoretical predictions and field observation.[1,2] On the other hand, turbulence with scales comparable to the size of the vortex core tends to promote bursting instability, which is most effective in destroying the swirl inside vortex wakes. As the vortex wake (two-dimensional or trailing) approaches the ground, the two primary vortices move sideways. Secondary vortices develop under the primary vortices because of flow separation inside the viscous boundary layer. The secondary vortices cause the primary vortices to rebound, which is not predicted by the inviscid theory.[9]

Atmospheric stability is another important parameter that affects the evolution of vortex wakes. Most of the early work was conducted to demonstrate the suppression of vortex-wake translation in a stably stratified fluid. Crow[10] predicted that, for high Froude numbers in weakly stratified fluids, acceleration of vortex-wake translation could result due to imbalance of the buoyancy between the fluids in the vortex cores and in the ambient. As a result, the vortex separation decreases and the vortex translation speeds up. In an attempt to validate Crow's prediction, Tomassian[11] conducted laboratory experiments using a two-dimensional vortex pair in a stratified towing tank. He observed an initial speedup of the vortex wake followed by a slow down at later time. Numerical simulations by Robins and Delisi,[12] Spalart,[13] and Garten et al.[14] showed that weak ambient stratification, $F \to 1$, caused a decrease in separation distance and subsequent acceleration of laminar two-dimensional vortex pairs, in general agreement with Crow's predictions and the initial acceleration phase observed in the experimental results by Tomassian.[11] Garten et al.[14] showed that acceleration ceased when diffusion of the vortex cores become dominant. There was no mention whether the numerical results show subsequent deceleration as observed by Tomassian.[11]

For trailing vortices generated by towed wings supported by thin struts, Sarpkaya and Johnson[15] showed no evidence of vortex acceleration due to the detrainment process predicted by Crow.[10] According to Donaldson and Bilinan,[16] it is possible that, for very clean wings with almost rectangular loading, the behavior predicted by Crow[10] may be observed for a short time. Numerical simulations by Robins and Delisi[17] and Garten et al.[18] also showed no acceleration of trailing vortex pairs. Garten et al.[18] indicated that Crow instability on trailing vortex pairs might dominate the evolution on a timescale that precludes the (two-dimensional) acceleration from occurring.

In this paper, the effects of ambient stratification on vortex wakes were investigated by conducting visualization experiments in a stratified towing tank. The main objective was to simulate the high-Froude-number regimes in which detrainment was expected to occur. Special efforts were made to create favorable environments and conditions to ensure that the detrainment phenomenon, if present, would not be masked or contaminated. For example, two-dimensional vortex pairs were generated by a specially designed vortex generator to alleviate an abrupt stop of the plunger at the end of its stroke, an undesirable feature that would generate a counter-rotating vortex pair to annihilate the movement of the primary vortex pair. Such a vortex generator was used successfully in studying the ground effects on vortex wakes.[8] For three-dimensional trailing vortex pairs, a towed rectangular wing suspended on fine wires was used to eliminate the strut wakes. The author has demonstrated that the trailing vortex wakes thus generated are very clean, allowing the

Received 23 April 2005; revision received 8 February 2006; accepted for publication 9 February 2006.

*Consultant Scientist. Associate Fellow AIAA.

observation of Crow's instability for a long time in both quiescent and turbulent ambient conditions.[7] Both brine (NaCl) and heat were used to prepare stably stratified fluids for a wide range of density gradients. Attempts were made to establish solid evidence of the presence (or absence) of detrainment at high Froude numbers and to study its generation and evolution. From the experimental results, the roles of detrainment in influencing the kinematics and dynamics of vortex wakes were assessed.

II. Relevant Parameters and Formulas

In a stably stratified fluid, one of the most important dynamic parameters is the internal Froude number, defined in dimensionless form as

$$F = U/NL \tag{1}$$

where U, N, and L are, respectively, the characteristic scales for the velocity, the Brunt–Väisälä (B–V) frequency, and the length. Here, the B–V frequency is the natural buoyancy frequency of the stratified flow:

$$N = \left(-\frac{g}{\rho_0}\frac{\mathrm{d}\bar{\rho}}{\mathrm{d}z}\right)^{\frac{1}{2}} \tag{2}$$

where g is the gravitational acceleration, z is the vertical coordinate, ρ is the density, and ρ_0 is a reference density. In the present context, the length and velocity scales are defined to be the initial vortex separation b_0 and initial vortex translation speed W_0. By definition, the Froude number is the ratio of the inertial force to the buoyancy force. In the literature, the inverse of F, $N^* = Nb_0/W_0$, is often referred to as the stratification parameter.[15]

The Reynolds number is defined as $Re = W_0 b_0/\nu$. In the literature, the Reynolds number is often defined in terms of the circulation, $\Gamma = 2\pi W_0 b_0$, so that $Re' = \Gamma/\nu = 2\pi Re$.

When $F \ll 1$, that is, buoyancy dominates the flow, the translation of the vortex wake is severely limited by the density stratification. A large portion of the kinetic energy in a vortex wake is converted into potential energy that radiates away from the source in the form of internal waves.[5] However, according to Hecht et al.,[19] the rolling moments induced on a following aircraft may persist even after the translation of the vortex wake stops. When $F \gg 1$, that is, inertial force dominates the flow, the buoyancy has little influence on the nonlinear dynamics of the motion.

Based on the assumption that b, the vortex separation, remains constant and that the effects of viscous and turbulent diffusion are negligible, Saffman[4] modeled the physics of the process and predicted the vortex wake oscillating in the stably stratified fluid:

$$h/b_0 = (1+c)^{0.5} F \sin[N^* t^*/(1+c)^{0.5}] \tag{3}$$

where c is a shape factor of the order of unity and $t^* = W_0 t/b_0$. Note that $N^* t^* = (Nb_0/W_0)(W_0 t/b_0) = Nt$. Equation (3) predicts a linear relationship between the maximum vertical translation $h_{\max}$ and the Froude number, $F = W_0/Nb_0$. For small cores with $c = 1.2$, we have

$$h_{\max}/b_0 = 1.48\,F \tag{4}$$

Laboratory and numerical results of the maximum vortex translation agree fairly well with the prediction by Saffman[4] for low F (Refs. 5, 15, and 19). For high F, the theory overpredicts the vortex translation. One of the reasons is that the theory does not take into consideration the effect of vortex instability and various demise mechanisms.[7,15,20]

For high F, Crow[10] predicted that the vortex translation speeds up as heavy fluid in the oval is detrained into the wake of the vortex pair and the vortex separation contracts. Crow's derivation led to an identical set of equations derived by Scorer and Davenport[21]:

$$h/b_0 = (8\pi/\sigma)^{0.5} F \sinh[(\sigma/8\pi)^{0.5} N^* t^*] \tag{5}$$

where $\alpha = 11.3$ according to Saffman.[4] Note that Eq. (3) predicts that the vortex wake reaches the maximum translation at $N^* t^* = 2.32$ or 0.37 B–V period. For the same F, h/b_0 predicted by Eq. (5) exceeds that predicted by Eq. (3) for $N^* t^* = Nt \le 0.5$, as the result of detrainment described by Crow.[10] For a trailing vortex wake, the effect of detrainment is expected to compete with that of the turbulent diffusion and vortex instability (linking or bursting), which becomes evident at large times. The effect of turbulent diffusion and vortex instability, however, are not taken into account in both theories. In reality, the slope of h/b_0 at large times levels off as the result of turbulent diffusion.

Tomassian[11] investigated the potential effects of detrainment on the motion of the vortex wake by releasing a two-dimensional vortex pair in a stratified fluid. The trajectories indicate that when stratification is dominating, the speed of the vortex pair initially increases, and its separation decreases in agreement with Crow's prediction. At a later time, deceleration and increased separation are observed that are opposite to the theoretical prediction. The phenomenon of slowdown and increased separation is attributed to two factors. The first factor is turbulent diffusion, which takes place whether the fluid is stratified or not. The second factor is the result of the production of countersign vorticity in the presence of stratification behind the original vortex pair. The net effect of the detrainment, even in the high F regime, is, therefore, rather small due to the interaction of the foregoing factors.

Using a delta wing model mounted on a thin strut and towed in a stably stratified fluid, Sarpkaya and Johnson[15] demonstrated that the maximum translation of the vortex wake asymptotically approaches that in a neutral environment ($F \to \infty$). Their results have suggested that the detrainment process, if present, has an insignificant effect on enhancing the vortex translation. It is not clear whether the disturbance induced by the strut could mask the apparently delicate effect of detrainment. According to Donaldson and Bilinan,[16] it is possible that for very clean wings with almost rectangular loading, tested in a truly quiescent medium, the behavior predicted by Crow[10] may be observed for a short time. Because the atmospheric boundary layer near ground level is often weakly stratified, the high F regime is relevant to the aircraft wake phenomenon. At present, the generation and evolution of the vortex wake in the high F regime is still not well understood. In particular, no direct evidence except indirect inference from vortex kinematics, that is, acceleration and deceleration of vortex trajectories, has been established for the presence of detrainment.

III. Experimental Methods and Laboratory Facility

Experiments were conducted in stratified towing tanks filled with stably stratified fluids.[7] Two methods were used to prepare stably stratified fluids in the tank, depending on the range of F for the runs; low-F runs would require a strongly stratified fluid and vice versa. A brine (NaCl) and heat were used as the sources for preparing a strongly and weakly stratified fluid in the tank, respectively. Clean vortex wakes were generated by a two-dimensional vortex generator and by a towed NACA 0012 wing model.[7,8] Fluorescent dyes illuminated with a laser sheet or ultraviolet lights were used to visualize the vortex wakes and to track their movements with still and movie cameras.

A. Towing Tank

The towing tank measures 18.3 m long, 1.2 m wide, and 0.91 m deep. It has glass sidewalls and a glass floor to permit visualization from all directions. The tank may be filled with either fresh water or stratified fluids to simulate a variety of atmospheric and oceanographic conditions. For studying vortex-wake phenomena, towing tanks are superior to wind tunnels. Vortex wakes generated in wind tunnels are swept away from the working section in a very short time whereas those generated in towing tanks can be observed for a long time until the wall effects become important. A detailed description of the towing tank and its special features are given elsewhere.[7,8,22]

B. Ambient Stratification

The towing tank was equipped with a special filling system to prepare a stratified fluid with a constant or nonuniform density

gradient.[7,23] For a relatively strong density gradient, stratification was made by first filling the tank with tap water at room temperature. Then, many layers of salt solution with increasing density, created by mixing tap water and concentrated salt brine stored in two head tanks, were fed through a set of filling channels on the bottom of the tow tank. Low-level mixing during feeding of the salt solution smoothed the sharp jump of density between layers, except for those with exceptionally large density differences. Further smoothing of the density profile took place during the settling period after the fluid is stratified. In about 2–3 h, a quiescent stratified fluid with an essentially constant density gradient was established (Fig 1). The density profile was measured with a single-electrode conductivity probe calibrated with salt solutions of known density.[22]

For weak stratification ($N < 0.09$ rad/s), the preceding method does not work well due to the mixing introduced during the feeding of the salt solution. A method of thermal stratification was subsequently developed and employed. After the tank was filled with tap water at room temperature, colder water was pumped into the bottom at one end of the tank and drained at a lower flow rate at the other end (Fig. 2). Excess water is drawn down through a surface drain. Mixing of the colder bottom fluid pumped into the tank and the warmer overlying fluid in the shear region, that is, the interface of the two fluids, resulted in a thermally stratified layer in the tank. The gradient of the stratification and the thickness of the stratified layer are controlled by the temperature differential of the two fluids and the flow rate of the colder fluid. This procedure enables us to achieve an extremely weak stratification. To eliminate large density jumps and achieve a fluid with a nearly constant density gradient or B–V frequency, limited vertical mixing was introduced by towing a rake with vertical aluminum bars (1-cm^2 cross section) through the tank at low speeds.

To obtain temperature profiles of the tow tank, we used three type T thermocouples (Sensortek IT-23; time constant 0.005 s) that have probes coated with a thin layer of wax to prevent deterioration in water. Two of the thermocouples were wired side by side in series to obtain a differential output, and the third thermocouple was mounted at middepth of the tank for monitoring the absolute tank temperature. The absolute temperature thermocouple output was sent directly to the termination panel of the computer. The outputs from the differential thermocouples were sent to an amplifier (Burr–Brown MPV99O) with a gain of 10,000 and then to the termination panel of the computer. The differential thermocouples were mounted on a traversing mechanism. Before performing a temperature profile in the tank, all three thermocouples were placed in a constant-temperature bath. The average absolute temperature was calibrated with a precision thermometer (0.1°C). The average value of the differential reading was used to correct for the temperature measurement in the tank.

Temperature profiles were measured just before and/or after the experiments. The differentia1 thermocouple was traversed from the surface to the bottom of the tow tank at 1 cm/s. Data were collected at 20 Hz for 70 s. The traverse was equipped with a cable displacement transducer to record the depth of the thermocouple relative to the positions of the two-dimensional vortex generator or the wing. The temperature at any given height was determined by adding the differential value to the average of the absolute temperature readings.

Figure 3 is a typical temperature profile. The density gradient of a temperature-stratified fluid cannot be controlled accurately, especially for very weak stratification. The average temperature gradient of the water column was used to calculate the density gradient.

The density of tap water at various temperatures is well established.[24] The relationship between the B–V frequency N and the temperature gradient $\mathrm{d}T/\mathrm{d}z$ can be derived with the water temperature as a parameter. Consider the profile in Fig. 3 with a mean temperature of about 19.1°C and an average temperature gradient of 0.0016°C/cm. This corresponds to a B–V frequency N of 0.018 rad/s. For a vortex pair with a separation of 8 cm and a translation speed of 0.8 cm/s, the Froude number is, therefore, 5.5.

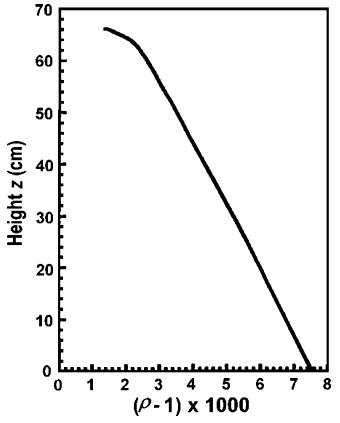

Fig. 1 Typical stratification profile in fluids prepared with NaCl brine.

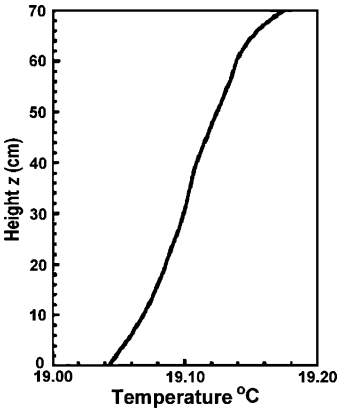

Fig. 3 Typical temperature pofile in weakly stratified fluid with nearly constant density gradient, $N \approx 0.018$ rad/s.

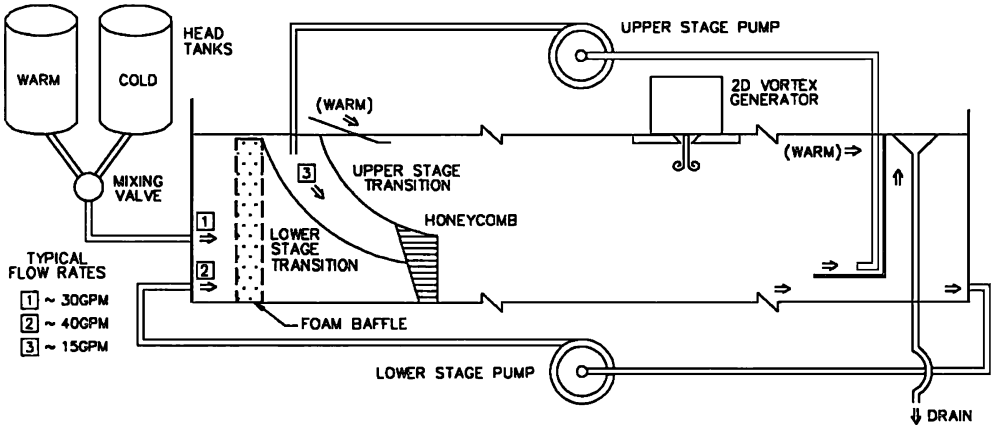

Fig. 2 Experimental setup for preparing thermally stratified fluid.

C. Two-Dimensional Vortex Generator

To study stratification and cross-shear effects on a vortex wake, a two-dimensional vortex generator that operates by squirting fluid out through a narrow slot was designed and constructed (Fig. 4). A special plunging mechanism using compressed air as the forcing medium was assembled to do away with a mechanical plunger that starts and stops impulsively. An impulsive stop creates a counter-rotating vortex pair that annihilates the motion of the primary vortex pair (Fig. 5a). The two-dimensional vortex pair thus generated differs from the trailing vortex pair from an aircraft. The present mechanism incorporated a ramp-down pressure stroke before stopping to alleviate the generation of the counter-rotating vortex pair (Fig. 5b).

Figure 4a shows the overall set up for the two-dimensional vortex generator. It consists of a sealed box (Fig. 4b) with a slot 5.7 cm wide on its bottom side; the edges of the slot have a 45-deg bevel. The box was made of aluminum with dimensions of 18 (width) × 32 cm (depth). The bottom of the box is submerged below the water surface, and the vortex pair is formed and exits from this slot. The water level in the box is lifted by means of a vacuum pump. A pressure line from a shop compressor is connected to a paint tank in which water is partially filled; a separate pressure line connects the paint tank and the generator box. The volume of water filled in the tank is inversely proportional to the pressure used to drive the generator. The ejection of fluid is controlled by two solenoid valves on the paint tank through a timing circuit. One valve is on the inlet to the paint tank, and the other is between the vortex box and the paint tank. Typically, the paint tank is pressurized to 20 psi (0.14 MPa). To trigger an event, a switch activates the timing circuit, which opens both solenoid valves. This initiates a strong continuous supply of air to force the fluid through the slot and then, after 2 s, the supply valve closes. This gradually halts the ejection by having the residual air in the paint tank gradually reducing to atmospheric level. After 15 s, the solenoid valve to the vortex box closes.

To trace the vortex pair, a fluorescent dye solution was mixed with water pumped slowly from the towing tank at the exit slot of the generator. The dilute dye solution was, therefore, neutrally buoyant with the stratified water at that level. As the dyed solution was squirted out the box to form the vortex pair, the vortex pair became visible in the presence of the fluorescent dye. A sheet of laser light generated by an oscillating mirror was used to illuminate the vortex pair. The plane of the laser sheet was oriented perpendicular to the axis of the vortex pair.[8,25]

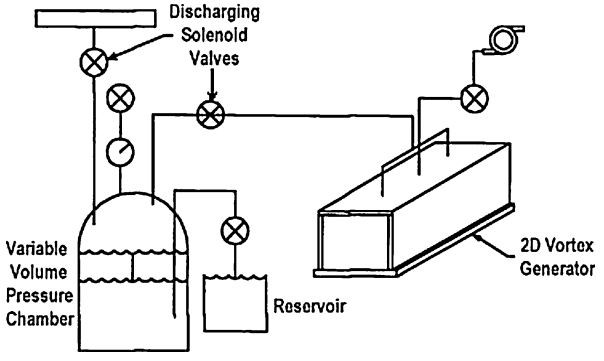

a) Experimental setup

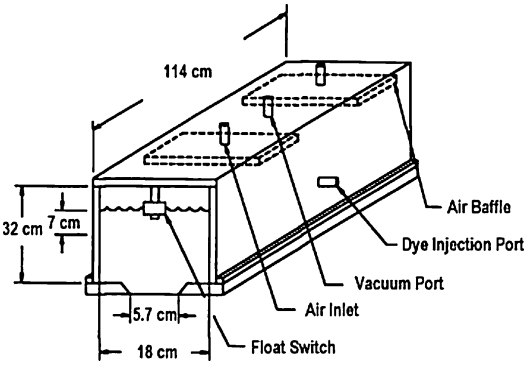

b) Details of two-dimensional vortex generator

Fig. 4 Schematic of two-dimensional vortex generator and experimental setup.

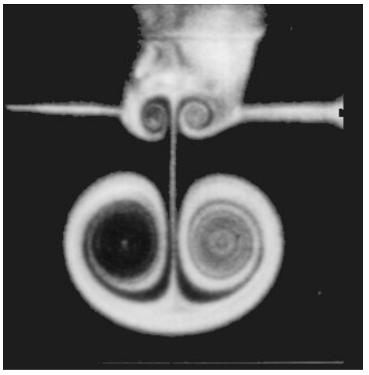

a) Presence of counter-rotating vortex pair

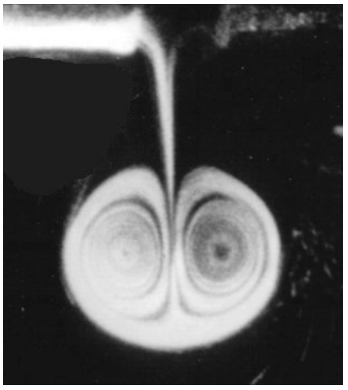

b) Absence of counter-rotating vortex pair

Fig. 5 Optimization of two-dimensional vortex generation alleviation of counter-rotating vortex pair due to impulsive stop of plunger at end of stroke.

D. Trailing Vortex Generator

The vortex wake was generated by towing a rectangular wing model (NACA 0012) along the length of the tank. The wing model has a 10.2-cm span and 5.1-cm chord. The maximum dimensions of the wing are dictated by the dimensions of the tow tank and the requirement that the water surface, the tank floor, and the tank walls do not interfere with the vortex phenomena to be investigated. For a towing speed of 40 cm/s, the chord Reynolds number is 2×10^4. The dimensionless tank depth and half-width based on b_0 are 10.5 and 7.5, respectively. For $h/b_0 < 6.5$ and $h/b_0 > 6.5$, the wing were placed 3.2 b_0 and 1.6 b_0 above the tank floor and the corresponding depths of submergence were 7.3 b_0 and 8.9 b_0, respectively. At $\alpha = -10$ deg and $U = 40$ cm, W_0 reduced from 1.1 to 0.8 cm/s as the wing/floor separation changed from 3.2 b_0 to 1.6 b_0. This effectively reduced the equivalent incident angle of the wing. According to Sarpkaya and Johnson,[15] such a reduction should not modify the dynamics of the vortex wakes significantly as long as W_0 was used in forming the dimensionless parameters.

A special mounting technique was used in which the wing was hung on three fine stainless-steel wires (0.008-cm diameter) at negative angles of attack, as shown in Fig. 6. This eliminated the strut or sting wake, which could interact with and contaminate the vortex wake during its evolution. The wing model was made of brass. In the working section where the carriage is moving at a constant speed, the wing maintains a steady posture without detectable swinging motion.

Just before a run, a very thin paste of fluorescent dye, for example, fluorescein disodium salt, mixed in corn syrup was applied to the

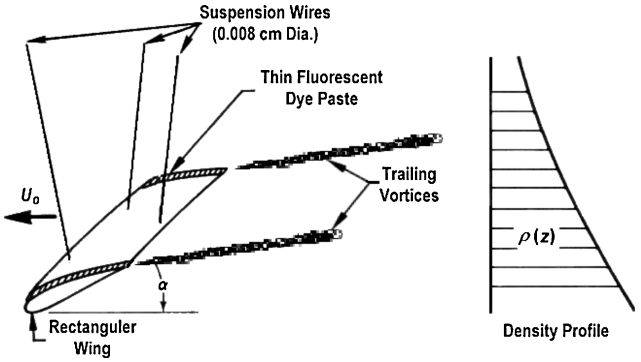

Fig. 6 Trailing vortices generated by towed wing model (NACA 0012) at negative angle.

two outer edges of the wing (Fig. 6). Two dyes of different colors were sometimes used on the two edges to provide a visual distinction between the two trailing vortices. During the roll up of the trailing vortices, the dye that washed away from the wing edges is trapped in the cores. For the side and top views, the vortex wake tracked by the fluorescent dye was illuminated with several banks of UV lights and a laser sheet light, respectively. The translation of the trailing vortex wakes was derived from the side view of the visual records acquired with a 16-mm movie camera. For all of the visual runs, a yardstick placed inside the tank was used to calibrate and correct image distortions, if needed, during image analysis and processing.

IV. Results and Discussion

As discussed in Sec. II, ambient stratification generally suppresses the motion and translation of the trailing vortex wakes. The maximum distance that a trailing vortex pair travels before breaking up is significantly reduced in a strongly (stably) stratified environment, that is, for small F. Most of the kinetic energy in the vortex cores is converted into potential energy in the form of internal waves radiated away through the stratified fluid. The internal wave motion is very slow and would essentially have no effect on even the smallest following aircraft. Therefore, the potential hazard to smaller aircraft by trailing vortex wakes generated by large transport aircraft is significantly reduced when the atmospheric boundary layer is strongly stratified. Furthermore, both theory[4] and numerical solutions[5,19] have predicted adequately the motion of the vortex pair for small F (Ref. 15). For large F (>2), however, the flow phenomena are complicated and not yet well understood. There are discrepancies among analytical, numerical, and laboratory results, as reviewed briefly in Sec. I.

As described in Sec. III, stratified fluids were prepared in the towing tank by means of brine and thermal stratification for strong and weak stratifications, respectively. Several series of experiments using the two-dimensional vortex generator and the NACA wing were then conducted over a wide range of values of F, with emphasis on $F > 2$ to examine the nonlinear vortex behavior and Crow's prediction of vortex acceleration resulting from detrainment.

A. Two-Dimensional Vortex Wake

To establish a reference, Fig. 7 shows sequential images of a two-dimensional vortex wake (cross-track vertical plane) in a homogeneous fluid, with $b_0 = 6.2$ cm, $W_0 = 1.65$ cm/s, and $F = \infty$. Time after release in seconds and the dimensionless time, $t^* = W_0 t/b_0$, (in parentheses) are shown in the lower-right-hand side of each image. The Reynolds number based on W_0 and b_0 is $Re = 1022$, or $Re' = 2\pi W_0 b_0/\nu = 6418$. A mirror placed on the bottom of the tank directed a laser sheet from lower left to upper right to illuminate a thin section of the vortex wake. A brightness gradient exists along the path of the laser sheet as a result of absorption of the laser light by the dye.

The image sequence shows that a nearly symmetric vortex pair exits the vortex generator and descends slowly into the ambient. Entrainment of ambient fluid (no dye) takes place predominantly

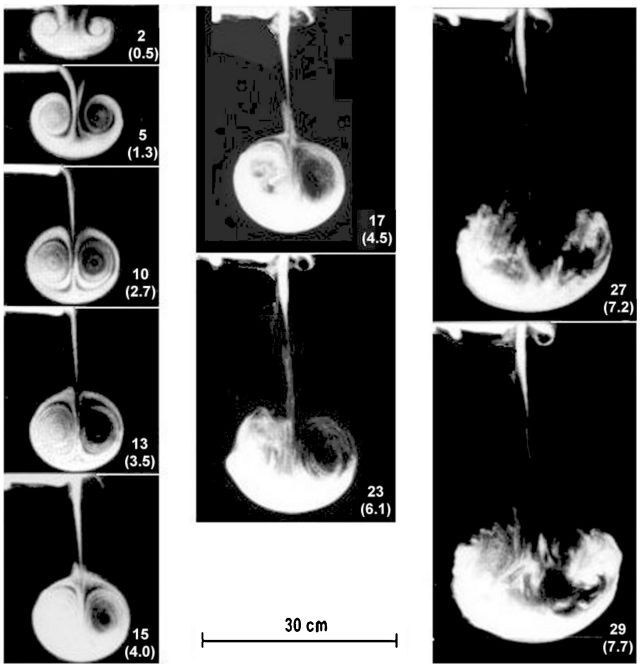

Fig. 7 Evolution of two-dimensional vortex pair in homogeneous fluid: $W_0 = 1.65$ cm/s and $b_0 = 6.2$ cm; numbers are time in seconds and dimensionless time (in parentheses).

at the downstream or tail end of the vortex wake. Initially, the entrained ambient fluid and the dye released from the vortex generator rolls into a swirl with alternating dark and bright bands ($t^* = 2.7$). Diffusion inside the vortex reduces the contrast between the two bands with time. At $t^* = 4.0$, the tail end of the vortex wake appears to become turbulent. In addition, self-induced instability further helps mixing the dye inside the vortex wake. As a result, the dye concentration in the tail end of the vortex wake is diluted, and it becomes decreasingly visible with time. This is particularly evident for $t^* > 4.5$. From the image sequence, the width of the oval in particular continues to increase. From the movie record, the evolution from a well-coherent vortex pair to a turbulent blob can be seen clearly. The turbulent blob continues to grow in size and descend slowly. Entrainment, turbulent diffusion, and self-induced instability are responsible for the deterioration of the swirl and, therefore, the decrease in the induced velocity of the vortices.

In strongly stratified fluids, stratification suppresses the vortex translation as reported by Tomassian.[11] In weakly stratified fluids, detrainment was predicted analytically and numerically.[10,13,14] A weak acceleration followed by a deceleration was implied indirectly from laboratory experiments.[11] There is, however, no visual or direct evidence that detrainment actually takes place either in the laboratory or in the field.

A series of experiments using the two-dimensional vortex generator was conducted in salt and thermally stratified fluids with an emphasis on visualizing the detrainment process and its effects on the vortex wake. Figure 8 shows the visual results from one of the runs in which detrainment clearly takes place. The corresponding key parameters are $b_0 = 5.0$ cm, $W_0 = 1.1$ cm/s, $F = 3.2$, and $Re = 550$ ($Re' = 3454$). Initially, the kinetic energy of the vortex pair dominates, and the stratification is not felt. The potential energy of the vortex wake increases along its path as a result of increase in the density difference between the fluid in the vortex wake and in the ambient. When the kinetic energy is overcome by the potential energy, a narrow plume initiates at the tail of the recirculation region around $t^* \approx 2.8$. The plume that consists of a pair of counter-rotating vortices slowly ascends all of the way to the exit plane of the generator. The counter-rotating vortices with strength considerably weaker than their primary counterparts are expected to have relatively small effects on the translation of the latter. The counter-rotating vortices move sideways as they approach the exit plane of the generator. A secondary vortex is generated between each of the vortices and the

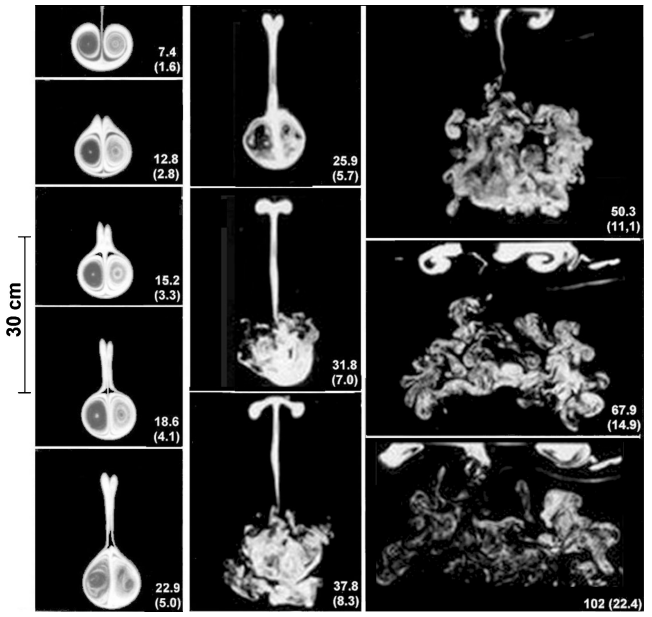

Fig. 8 Detrainment observed from two-dimensional vortex pair released into stratified fluid with temperature gradient of 0.025°: $W_0 = 1.1$ cm/s, $b_0 = 5.0$ cm, and $F = 3.2$.

exit plane as the result of viscous–inviscid interaction in the boundary layer. The initial formation of the secondary vortices cannot be clearly visualized in the absence of dye, $t^* \approx 7.0$–8.3. Their presence becomes increasingly evident as dye is entrained into them at later time, $t^* \approx 11.1$–22.4. The induced velocity by the secondary vortices causes the counter-rotating vortices to rebound, the "ground effect" demonstrated by Liu et al.[8]

The primary vortex wake continues to descend. At $t^* \approx 2.8$, the fluid in the outer recirculation region that reaches the tail of the vortex wake is overcome by the buoyancy force, reverses its normal downward course, and forms the detrainment plume. Before the formation of the plume, entrainment of the ambient fluid (no dye) is evident, $t^* = 1.6$. The dark and light bands appeared in the vortex wake corresponding to the fluids entrained from the ambient and released from the vortex generator, respectively. Such a pattern persists until $t^* = 4.1$ or longer. At $t^* = 2.8$, the two small dark pockets located between the vortex cores and the ascending plume are a small amount of trapped ambient fluid. These pockets mark the initial basis separating the primary vortex wake and the ascending plume. Below the pockets, the fluid continues swirling in the two vortex cores. The pockets merge into one around $t^* = 5.0$, at which time the swirl in the vortex cores has deteriorated. The pocket begins to ascend very slowly with the plume. None of the fluid in the plume above the pockets is from the inner recirculation regions. Apparently, only the fluid in the outer recirculation region works against the buoyancy force and feeds into the plume.

Once detrainment is initiated, entrainment of the ambient fluid is blocked by the column of the detraining fluid. As can been seen from the images from $t^* = 2.8$ to 5.7, no ambient fluid is being entrained into the vortex wake. The lack of entrainment of ambient fluid into the vortex wake delays the growth in the width of the vortex wake, which would otherwise slow down the vortex translation as is observed in the homogeneous run (Fig. 7). Entrainment of the ambient fluid may resume after the vortex wake bursts at around $t^* = 7.0$, and feeding of fluid into the detrainment plume ceases.

The vortex cores have become somewhat disorganized and burst into a turbulent blot at around $t^* \approx 5.0$ and 7.0, respectively. In contrast to the run for $F \to \infty$, the disorganization is predominantly caused by self-induced instability and turbulent diffusion rather than by entrainment that is suppressed by stratification and detrainment. As such, the growth in the size of the vortex wake, particularly its width, slows down.

The vortex wake carried by inertia overshoots its equilibrium position. The turbulent blob consisting of the original fluid (with dye) in the vortex wake and the entrained fluid (no dye) from the ambient begin to rebound at $t^* > 8.3$ or a 0.41 B–V period under the influence of the buoyancy force. Note that the wakes of a towed slender body and sphere reach maximum height at about 0.75 and 0.32 B–V periods, respectively.[23,26] Subsequently, the vortex wakes spread sideways because the vertical spread is inhibited by the ambient stratification. Similar patterns were observed for the cases with higher F (not shown). The intensity of detrainment, however, weakens for $F > 4$.

The formation and evolution of the plume just described positively identifies the detrainment phenomenon predicted by Crow.[10] However, careful examination of the sequential images in Fig. 8 and in the movie record shows that there is a discrepancy in the behavior between the laboratory results and Crow's prediction. The detrainment plume observed in the laboratory results is predominantly from the fluid contained in the outer edge of the recirculation region or the outer recirculation region. Initially, the inertia force dominates and the vortex wake moves downward, similar to that of the run conducted in the homogeneous fluid where the counter-rotating motion in the vortex wake experiences no resistance. As shown in Fig. 8, the vortex wake moves downward by the mutually induced velocity. The downward movement slows down by various demise mechanisms (entrainment, vortex instability, and turbulent mixing) in the real fluid.[15]

The inertia of the swirl maintains the counter-rotating motion that continues driving the vortex wake downward into the stratified ambient. Meanwhile, the outer recirculation region continues to lose fluid and feed the plume as the vortex wake descends, even after the vortex cores become disorganized and turn into a turbulent blob in the range $7.0 < t^* < 8.3$. During that process, the vortex wake is reshaped into a teardrop formation around $t^* = 5.0$. In other words, the growth in the ascending plume takes place at the expense of the increase in the width of the vortex wake. One of the direct consequences of detrainment is that the overall potential energy buildup inside the vortex wake is reduced as part of the fluid in the outer recirculation region continuously feeds into the ascending plume.

Because the detrainment is not from the vortex cores, little or no contraction of the vortex separation is observed from the image sequence. The visual results do not support Crow's prediction that detrainment of fluid from the vortex cores results in contraction of the vortex separation, leading to acceleration of the vortex translation.

Selected outlines of the vortex wake and detrainment plume for $F = 3.2$ are superimposed onto the images of the vortex wake for $F \to \infty$ in Fig. 9 to facilitate direct comparison of the evolution

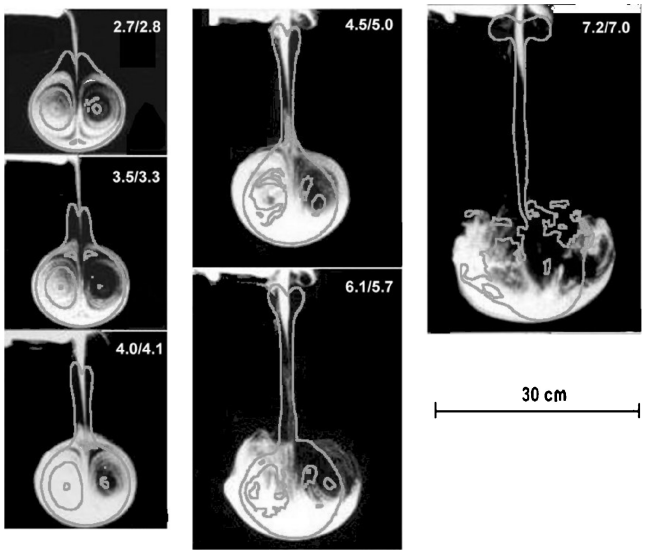

Fig. 9 Superimposition of selected outlines of vortex wake and detrainment plume for $F = 3.2$ onto vortex wake for $F \to \infty$ at about the same t^*; numbers in each frame are t^* for $F \to \infty$ and 3.2.

of their geometry at comparable t^*. The outlines are rescaled by a factor equal to the ratio of b_0, or 1.36 for the two runs, to match the geometry of the vortex wakes in earlier times. Figure 9 shows that the width of the vortex wake for $F \to \infty$ grows faster than that for $F = 3.2$. For example, the width has grown 41% at $t^* = 6.1$ for $F \to \infty$ and only 3% at $t^* = 5.7$ for $F = 3.2$.

In the stratified ambient, however, the potential energy of the vortex wake builds up as it moves downward. Based on the preceding description, the flow patterns before and after the formation of the detrainment plume are shown in Fig. 10. Note that the flow pattern of the vortex wake released in a homogeneous fluid is similar to that shown in Fig. 10a.

The visual results in Figs. 7 and 8 were digitized to derive the trajectories of the two-dimensional vortex wakes for $F \to \infty$ and $F = 3.2$, respectively. Figure 11 presents the trajectories of the two runs together with that predicted by the inviscid theory. The abscissa and ordinates are the dimensionless time $W_0 t/b_0$ and vertical vortex translation h/b_0, respectively. Initially, the trajectories for both F agree well with that predicted by the inviscid theory. As $W_0 t/b_0$ increases, the trajectory for $F \to \infty$ begins to slow and falls below the invicsid prediction. Although no visual data are available beyond $W_0 t/b_0 = 7.7$ for this run, there is much evidence in the literature that the trajectory continues rising with decreasing speed of the vortex translation.[1] The various demise mechanisms that are not accounted for in the inviscid theory are responsible for slowing down the vortex translation. As discussed, entrainment is the dominating factor for this case. For $F = 3.2$, the trajectory follows closely the inviscid prediction before slowing. Subsequently, the trajectory reaches its maximum translation and begins to rebound at $W_0 t/b_0 \approx 8$. Because no detrainment of fluid from the vortex cores and no noticeable contraction in the vortex separation are observed, the relatively small difference between the trajectories for $F \to \infty$ and $F = 3.2$ is not attributed to acceleration of the vortex translation. Instead, direct and indirect effects of detrainment delay the slowdown of the vortex translation experienced in the homogeneous run. Detrainment of fluid from the outer recirculation region and blockage of entrainment into the vortex wake effectively delay the onset of various demise mechanisms responsible for slowdown of the vortex translation. In addition, continuous detrainment of fluid from the outer recirculation transforms the vortex wake into a teardrop shape (Fig. 8, $t^* = 5.0$), which experiences lower drag than does the growing oval (Fig. 7, $t^* = 6.1$). Evidently, the difference in the shape of the two vortex wakes is partially responsible for the difference in the trajectories of the homogeneous and high-F runs.

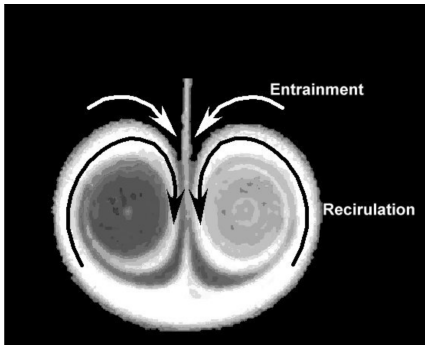

a) Before initiation of detrainment

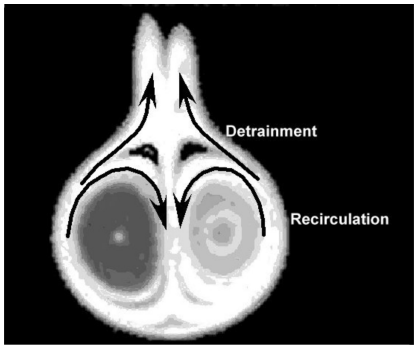

b) After initiation of detrainment

Fig. 10 Effect of detrainment on evolution of flow patterns around two-dimensional vortex wake for $F = 3.2$, blockage of entrainment.

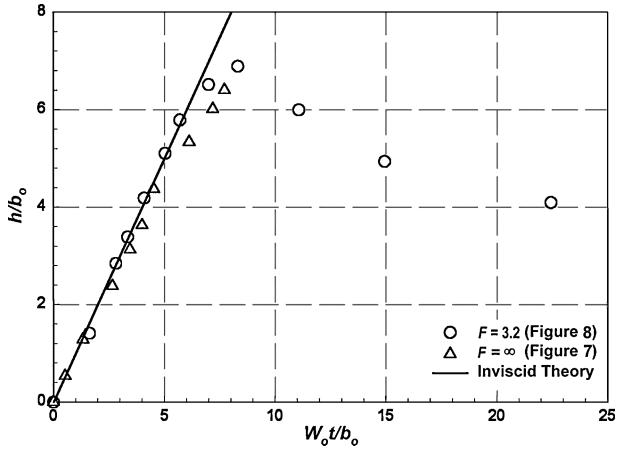

Fig. 11 Trajectories of two-dimensional vortex wakes in homogeneous and stratified fluids at high froude numbers.

The vortex wake for $F = 3.2$ overshoots its equilibrium position and finally undertakes a vertical oscillation in the stratified water column. The maximum frequency of oscillation corresponds to the B–V frequency. Such an oscillation is observed long after the breakup of the vortex wake. The movie record shows that the motion of the vortex wake also generates internal waves in the stably stratified fluid. In other words, part of the kinetic energy in the vortex wake is converted into potential energy and radiates away from its source in the form of interna1 waves.

The absence of acceleration in the vortex translation of the present results differ from those determined by Tomassian[11] and numerical solutions.[12–14] Tomassian[11] reported that acceleration of the vortex translation is observed at an early time, $t^* \sim 1.5$ and 3.5, depending on the value of F. He attributed the acceleration to detrainment that leads to contraction of the vortex separation. For $t^* > 3.5$, the translation decelerates, and the trajectories cross over the inviscid line and subsequently the trajectory for $F \to \infty$. Tomassian[11] attributed the subsequent slowdown to turbulent mixing and diffusion, which are not considered in Crow's theory.[10] Comparison of the two data sets in Fig. 11 shows that the vortex translation follows, but does not climb above, the inviscid curve for a longer time for $F = 3.2$ than for $F \to \infty$. There is a crossover of the trajectories between the two runs. The crossover is, however, the result of the buoyancy effect as the vortex wake overshoots its equilibrium position and oscillates near the B–V frequency of the ambient stratified fluid. Note that the intensity of turbulent mixing is weaker for $F = 3.2$ than for $F \to \infty$. Although a counter-rotating vortex pair is observed in the detrainment plume, its effects on the primary vortex wake are expected to be weak because of the large differences in size and vorticity (Fig. 8). It would be interesting to find out whether the predicted acceleration of the vortex translation for two-dimensional simulation disappears when the observed detrainment/entrainment mechanisms reported herein are modeled accordingly.

B. Trailing Vortex Wakes

For trailing vortex wakes generated by wings, however, no noticeable effect of detrainment has been reported from laboratory results.[15,27] According to Donaldson and Bilanin,[16] it is possible that detrainment, an inviscid phenomenon, may be observed for a very clean wing for a short time.

Previous experiments using a NACA 0012 wing model mounted on thin suspending wires (Fig. 6) instead of struts/stings has demonstrated that the vortex wakes thus generated were very clean.[7,8] Such a setup facilitated investigation of the generation and evolution of

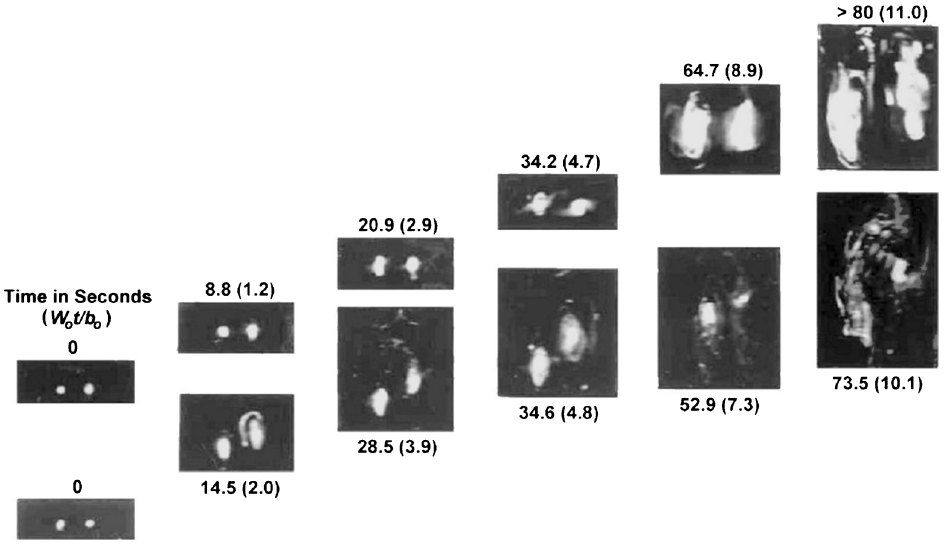

Fig. 12 End views of two trailing vortex wakes in homogeneous fluid; top and bottom sequences are in quiescent and weakly turbulent environments, respectively.[7]

Crow's instability and the ground effects in great detail.[20] Therefore, a series of experiments using the same wing was conducted in stratified fluids. Stratification was prepared with salt brine and heat for the low- and high-F cases. The specific goal was to determine whether detrainment takes place for three-dimensional trailing vortices and, if so, what its effects are on the vortex dynamics and kinematics. The trailing vortices were visualized by illuminating the flowfield with several banks of UV fluorescent lights from the side (side view) and with a sheet of laser light in the cross-track plane (end view), respectively. The vortex translation was measured by averaging over a 1.5-m section of the trajectory as viewed from the side window. Figure 12 shows the end view of two such vortex wakes in quiescent and weakly turbulent environments, respectively.[7]

Visual results of towed experiments using the clean wing do not show detrainment over a wide range of F from 0.69 to ∞. It turns out that the difference in tagging the trailing vortices and the two-dimensional vortex pair with fluorescent dye was responsible for the absence of detrainment observed in the trailing vortices for high F. As described in Sec. III, the fluid in the vortex generator was premixed with the fluorescent dye just before the two-dimensional vortex pair was generated. The entire vortex pair, including both the inner and outer circulation regions, was filled with the dye from the very beginning (Fig. 5). As a result, detrainment of the lighter fluid from the vortex pair (with dye) into the ambient (no dye) and entrainment of the heavier ambient fluid into the vortex pair can be visually observed as soon as they occur (Fig. 8). On the other hand, the dye washed away from the side edges of the wing model was initially entrained into the tight vortex cores but not the outer recirculation region (Fig. 12, $t^* = 0$). From Fig. 8, the estimated dimensionless time at which detrainment of the two-dimensional vortex pair first appears is $t^* = 2.8$. At about the same t^*, Fig. 12 shows that the dye is still very much confined in the center of the vortex cores, even when the ambient is weakly turbulent. For trailing vortices, any detrainment, unless from the dyed vortex cores, cannot be detected by pasting dye onto the edges of the wing.

Figure 13 shows the trajectories of the vertical translation of the trailing vortex wake. The solid curve corresponds to inviscid theory. It can be clearly seen that the trajectory for $F \to \infty$ serves as an asymptote to the cases of low F. No noticeable acceleration of the vortex translation is observed at high F. The trajectories for $F = 3.42$ and 5.48 are slightly higher than that for $F \to \infty$ because the vortex wakes overshoot their equilibrium positions before starting the oscillation. Such a trend is similar to that observed in the laboratory[15,27] and generally agrees with numerical solutions.[17,28]

Although there is no visual verification of detrainment for trailing vortex wakes at high F, there are two possible scenarios: 1) detrainment is absent or 2) detrainment is present but no fluid is detrained from the vortex cores. The second scenario is consistent with the findings for two-dimensional vortex wakes. The trajectories of trailing vortex wakes for $F = 3.42$ and 5.48 show a similar trend, but are not as noticeable as that of two-dimensional vortex wakes for $F = 3.2$. Based on such a similar trend and the visual evidence of detrainment in two-dimensional vortex wakes, it appears that relatively weak detrainment could have taken place for trailing vortex wakes. Visual verification of the presence of detrainment would, however, require a different visualization method.

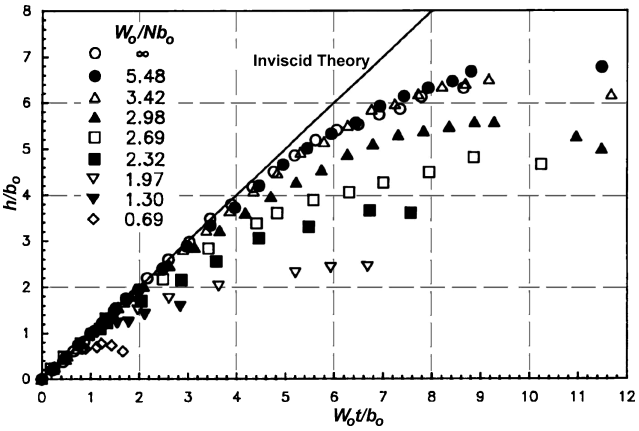

Fig. 13 Trajectories of trailing vortex wakes in homogeneous and stably stratified fluids.

Figure 14 shows the maximum vertical translation of trailing vortex wakes as a function of F (open diamonds) together with those of Sarpkaya and Johnson[15] (solid squares), who used a sharp-edged delta wing model with an apex angle of 50 deg, a base width of 12.6 cm, and an aspect ratio of 1.69 (solid squares). There is a reasonable resemblance in the trend of the two data sets, although the configurations of the two wing models are different. Of interest is the large difference in the asymptotic values of $h_{\max}/b_0$ for the two data sets (6.9 and 4.64). The large asymptotic value of $h_{\max}/b_0$ of the present work is partly attributed to the cleanness of the strut-free NACA 0012 wing used in the present experiments. For the same delta wing model with round tips, Sarpkaya[27] showed that the asymptotic value increased to 6.1.

The solid line in Fig. 14 is the two-dimensional prediction by Saffman.[4] For $F \leq 2.6$, the prediction agrees fairly well with both sets of data. The results by Sarpkay and Johnson[15] hover around

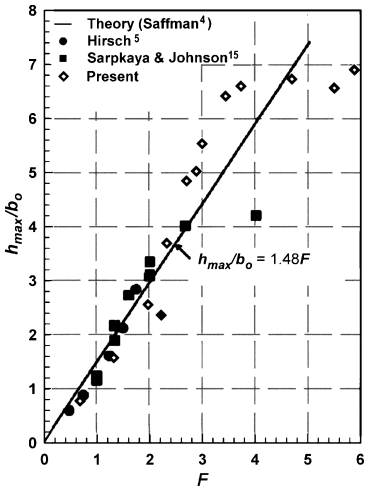

Fig. 14 Maximum vortex translation in stably stratified fluids.

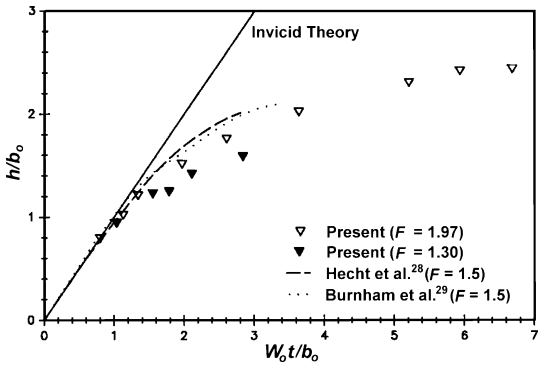

Fig. 15 Comparison of experimental results and numerical prediction of vortex trajectories.

the predicted line but drop below the line for $F > 2.6$ (one data point only). For small F, buoyancy dominates vortex dynamics, and the sole effect is to suppress the translation of the vortex wake. According to Sarpkaya,[27] various demise mechanisms (entrainment, vortex instability, and turbulent mixing) that are not considered in the theory begin to develop for large F. Therefore, disagreement between the theory and the experiments is anticipated.

The present results show that $h_{\max}/b_0$ climbs above and then drops below the predicted line at $F \approx 2.4$ and 4.6, respectively. The difference in $h_{\max}/b_0$ maximizes at $F \approx 3.4$. The disagreement again suggests that detrainment similar to, but not as strong as, that of two-dimensional vortex wakes is at play. The symptoms associated with detrainment of two-dimensional vortex wakes such as reduction in potential energy buildup and suppression of entrainment of ambient fluid into vortex cores are also applicable to trailing vortex wakes. The symptoms delay the development of demise mechanisms responsible for slowing down the vortex translation. Overshooting of vortex wakes from their equilibrium positions further increases $h_{\max}/b_0$. Apparently, detrainment only occurs within the relatively narrow range of F, with its strength maximized around the middle of the range. For $F > 4.5$, the crossover between the present results and the predicted line indicates that either detrainment or its effect has disappeared. The dynamics and kinematics of vortex wakes approach those of the asymptotic state for $F \to \infty$. As a result, various demise mechanisms dominate once again.

By using an inviscid numerical model with the Boussinesq approximation, Hirsh[5] demonstrated that numerical predictions (Fig. 14, solid circles) agree reasonably well with experiments for F as large as 1.75. No prediction was made beyond $F = 1.75$. The adequacy of the inviscid theory is in question in the absence of a turbulence model to handle dissipation, diffusion, and detrainment mechanisms in a real fluid.

Hecht et al.[19,29] developed a two-dimensional finite difference computer program with the incorporation of a second-order-closure

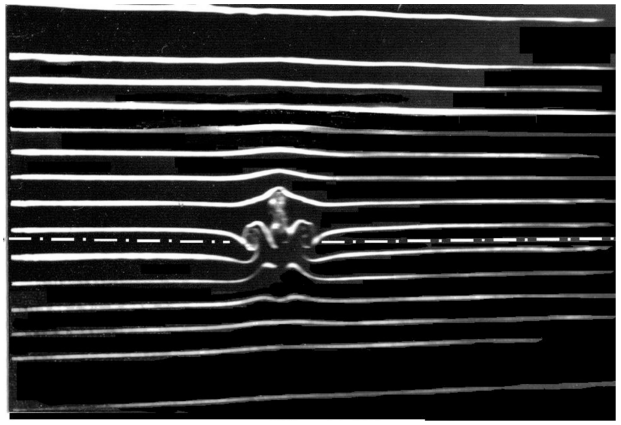

a) $Nt = 0.15$

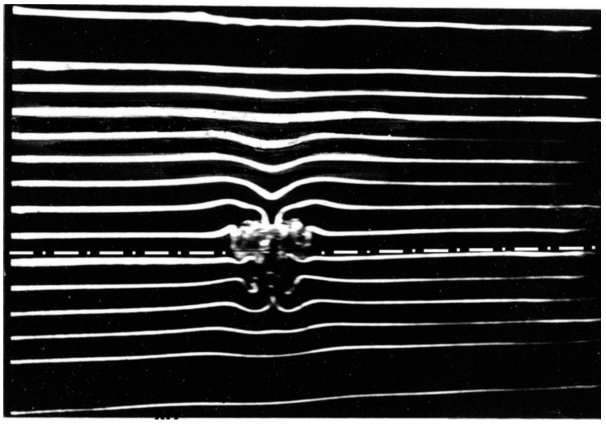

b) $Nt = 0.61$

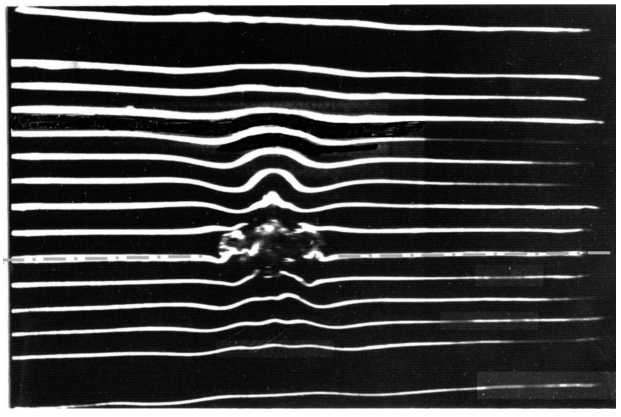

c) $Nt = 1.3$

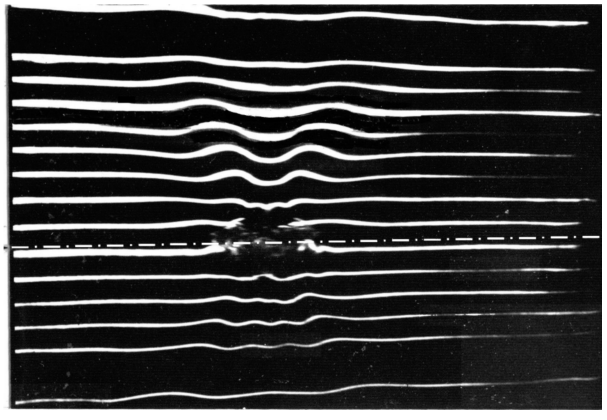

d) $Nt = 1.9$

Fig. 16 Internal waves generated by towed wing for $F = 0.01$: - - - - - -; submergence depth of wing.

turbulence model to predict the behavior of a vortex pair in a stratified atmosphere. For $F = 1.5$, the numerical prediction compares well with the field observation of a turbulent vortex descending in a stable atmosphere.[30] Figure 15 shows the comparison of the present results for $F = 1.97$ and 1.30, the numerical prediction by Hecht et al.,[29] and the corresponding field observation.[30] The numerical prediction and the field observation are slightly above the experimental results between $W_0 t/b_0 = 1.5$ and 3.5. This is as good an agreement as we would expect due to significant differences in the body shape and size and in the operational conditions. Note that $F = 1.5$ is relatively low, and the inviscid prediction is still applicable. It is imperative that the verification of numerical models is conducted in high-F regimes, where a delicate balance between detrainment and demise mechanisms of vortex wakes must be taken into account.

There have been several comments about the conversion of the kinetic energy of the vortex wake into potential energy through generation of internal waves that radiate away from the vortex wake. Figure 16 shows four cross-track images of the flowfield generated by the towed wing for $F = 0.01$ at $Nt = 0.15$, 0.61, 1.5, and 1.9 B–V periods, respectively. Visualization experiments were conducted using a fluorescent dye-layer method with a laser sheet to illuminate a cross-track plane.[31] In this series of experiments, the goal was to visualize the internal-wave field, and dye was not pasted on the edges of the wing to tag the trailing vortex wake. Dye entrained from dye layers in and near the path of the wing helps to identify the vortex wake. The movement of the vortex wake can also be tracked from those of surrounding dye layers. Figure 16 was selected to illustrate several key stages and the interaction of the vortex wake and internal waves. In the early stage, $Nt = 0.15$ B–V period, the vortex wake generated by passage of the wing rises as if the ambient fluid is homogeneous (Fig. 16a). As the vortex wake continue to rise, the buoyancy force becomes increasingly important. The vortex wake overshoots its equilibrium position and begins to collapse. At $Nt = 0.61$ B–V period, the collapsing vortex wake returns to its initial position and continue to descend (Fig. 16b). Internal waves generated by the towed wing and by the vortex wake propagate away from their sources. After the vortex wake descends to its minimum position, it reverses its course and returns to the initial position once again at $Nt = 1.3$ B–V periods (Fig. 16c). The visual results show that the vortex wake takes about 1.3 B–V periods to complete the first cycle of oscillation. The vortex wake continues oscillating with decreasing amplitude in the stratified fluid. Meanwhile, internal waves are generated by the motion of the vortex wake and propagate away (Fig. 16d). The internal-wave field can be divided into two components: Steady internal waves that are stationary with respect to the wing-fixed coordinates are generated by the passage of the towed wing. The unsteady or random internal waves that are not stationary with respect to the wing-fixed coordinates are generated by the motion of the vortex wake and oscillation. Steady and unsteady internal waves generated by towed cylinders were investigated by Liu.[31]

V. Summary

This paper presents the first ever visualization of detrainment phenomenon in vortex wakes at high Froude numbers. Since the phenomenon was predicted by Crow in 1974, there has been no direct physical evidence verifying its existence (or nonexistence) either from laboratory or field experiments.[10] The requirement for a very high Froude number does not occur often in the atmosphere, and conducting field experiment to visualize the trailing vortices is difficult and expensive. On the other hand, preparing a weakly stratified fluid in the laboratory to achieve the high-Froude-number conditions required for detrainment to take place is very difficult. The physical verification that detrainment does take place as predicted by Crow is an important discovery, although there are discrepancies between the observed and predicted results.

Visual experiments were conducted to investigate the kinematics and dynamics of two-dimensional and trailing vortex wakes in stratified fluids. The visual results were digitized to derive the trajectories of the vortex wakes to determine the effects of detrainment on the vortex translation. The detrainment phenomenon for two-dimensional vortex wakes generated by a specially designed two-dimensional vortex generator was identified. For high-Froude-number runs, weakly stratified fluids were prepared via temperature rather than brine stratification. For $F = 3.2$, a detrainment plume is initiated from the tail of the recirculation region at around $t^* \approx 2.8$ (Fig. 8). Fluid in the outer recirculation region only, but not in the inner recirculation (or the vortex cores), feeds into the detrainment plume. This observation is different from the scenario suggested by Crow.[10] Consequently, the vortex separation does not contract noticeably, and little or no acceleration of the vortex translation results, as opposed to the prediction by Crow.[10] The trajectories derived from the visual results show that the vertical translation of the two-dimensional vortex wake for $F = 3.2$ is closer to (but not above) the invicid theory than that for $F \to \infty$ (Fig. 12). It turns out that the detrainment plume, once initiated, blocks the ambient fluid from entraining into the vortex wake (Fig. 8). On the other hand, ambient fluid in the homogeneous run is entrained continuously into the vortex wake leading to noticeable growth in the wake width (Fig. 7). In the absence of entrainment, the stratified vortex wake reshapes into a teardrop configuration with little growth in the wake width as the outer recirculation continues losing fluid to the detrainment plume. Therefore, the drag on the teardrop-shaped stratified wake is lower than that of its homogeneous counterpart. The stratified wake overshoots its equilibrium position, reaches the maximum translation, and begins oscillating in the stratified fluid. There is a crossover between the two trajectories as the homogeneous wake continues translating in the same direction without reversal.

Clean trailing vortex wakes were generated by towing a NACA 0012 wing suspended on three fine wires. Visualization of vortex wakes was facilitated by pasting fluorescent dye on the edges of the wing. Visual results fail to verify the presence the detrainment phenomenon. It was discovered that fluorescent dye initially entrained and trapped into the tight vortex cores only diffuses very slowly outward. Detrainment similar to that of two-dimensional vortex wakes, if present, could not have been visually observed because of the absence of dye in the outer recirculation region. Trajectories of trailing vortex wakes for $F = 3.42$ and 5.48, however, demonstrate a symptom of a relatively weak detrainment consistent with that observed for two-dimensional vortex wakes. Supported by the strong evidence that detrainment does occur, but does not result in vortex contraction and acceleration as predicted by Crow[10] at high Froude numbers for two-dimensional vortex wakes, such a symptom strongly suggests that detrainment could also occur, but with a relatively weak strength, for trailing vortex wakes. The notion that detrainment takes place for both two-dimensional vortex wakes and trailing vortex wakes, but with no vortex acceleration, is consistent with other laboratory results, except for the momentary acceleration of two-dimensional vortex wakes reported by Tomassian.[11] It would be interesting to find out whether vortex acceleration would disappear in the two-dimensional numerical simulations by taking into account the detrainment process observed in the present work.

Acknowledgments

This work, conducted at Flow Research, Inc., was sponsored by the Transportation Systems Center, U.S. Department of Transportation, under Contract DTRS-57-87-C-00109, and by an Independent Research and Development fund from StereoVision Engineering. The author thanks R. A. Srnsky for carrying out the experiments.

References

[1]Tombach, I., "Observations of Atmospheric Effects of Vortex Wake Behavior," *Journal of Aircraft*, Vol. 10, No. 11, 1973, pp. 641–647.

[2]Crow, S. C., and Bate, E. R., Jr., "Lifespan of Trailing Vortices in a Turbulent Atmosphere," *Journal of Aircraft*, Vol. 13, No. 7, 1976, pp. 476–482.

[3]Bilanin, A. J., Teske, M. E., and Hirsh, J. E., "Neutral Atmospheric Effects on the Dissipation of Aircraft Vortex of Aircraft Vortex Wakes," *AIAA Journal*, Vol. 16, No. 9, 1978, pp. 956–961.

[4]Saffman, P. G., "The Motion of a Vortex Pair in a Stratified Atmosphere," *Journal of Applied Mathematics*, Vol. 52, 1972, pp. 107–119.

[5]Hirsh, R. S., "A Numerical Simulation of Vortex Motion in a Stratified Environment and Comparison with Experiments," *Johns Hopkins*

Applied Physics Laboratory Technical Digest, Vol. 6, No. 3, 1985, pp. 203–210.

[6]Greene, G. C., "An Approximate Model of Vortex Decay in the Atmosphere," *Journal of Aircraft*, Vol. 23, No. 7, 1986, pp. 566–573.

[7]Liu, H.-T., "Effects of Ambient Turbulence on the Decay of a Trailing Vortex Wake," *Journal of Aircraft*, Vol. 29, No. 2, 1992, pp. 255–263.

[8]Liu, H.-T., Hwang, P. A., and Srnsky, R. A., "Physical Modeling of Ground Effects on Vortex Wakes," *Journal of Aircraft*, Vol. 29, No. 6, 1992, pp. 1027–1034.

[9]Lamb, H., *Hydrodynamics*, 6th ed., Dover, New York, 1945.

[10]Crow, S. C., "Motion of a Vortex Pair in a Stably Stratified Fluid," Poseidon Research, Rept. 1, Los Angeles, May 1974.

[11]Tomassian, J. D., "The Motion of a Vortex Pair in a Stratified Medium," Ph.D. Dissertation, Engineering Dept., Univ. of California, Los Angeles, 1979.

[12]Robins, R. E., and Delisi, D. P., "Numerical Study of Vertical Shear and Stratification Effects on the Evolution of a Vortex Pair," *AIAA Journal*, Vol. 28, No. 4, 1990, pp. 661–669.

[13]Spalart, P., "On the Motion of Laminar Wing Wakes in a Stratified Fluid," *Journal of Fluid Mechanics*, Vol. 327, 1996, pp. 139–160.

[14]Garten, J. F., Arendt, S., Fritts, D. C., and Werne, J., "Dynamics of Counter-Rotating Vortex Pairs in Stratified and Sheared Environment," *Journal of Fluid Mechanics*, Vol. 361, 1998, pp. 189–236.

[15]Sarpkaya, T., and Johnson, S. K., "Trailing Vortices in Stratified Fluids," Naval Postgraduate School, Rept. NPS-69-82-003, Monterey, CA, June 1982.

[16]Donaldson, C. duP., and Bilanin, A. J., "Vortex Wakes of Conventional Aircraft," AGARDograph AG-204, AGARD, May 1975.

[17]Robins, R. E., and Delisi, D. P., "Numerical Simulations of Three-Dimensional Trailing Vortex Evolution," *AIAA Journal*, Vol. 35, No. 10, 1997, pp. 1552–1555.

[18]Garten, J. F., Werne, J., Fritts, D. C., and Arendt, S., "Direct Numerical Simulations of the Crow Instability and Subsequent Vortex Reconnection in a Stratified Fluid," *Journal of Fluid Mechanics*, Vol. 426, 2001, pp. 1–45.

[19]Hecht, A. M., Bilanin, A. J., Hirsh, J. E., and Snedeker, R. S., "Turbulent Vortices in Stratified Fluids," *AIAA Journal*, Vol. 18, No. 7, 1980, pp. 738–746.

[20]Crow, S. C., "Stability of Theory for a Pair of Trailing Vortices, *AIAA Journal*, Vol. 8, No. 12, 1970, pp. 2172–2179.

[21]Scorer, R. S., and Davenport, L. J., "Contrails and Aircraft Downwash," *Journal of Fluid Mechanics*, Vol. 43, No. 3, 1970, pp. 451–464.

[22]Liu, H.-T., "Energetics of Grid Turbulence in a Stably Stratified Fluid," *Journal of Fluid Mechanics*, Vol. 296, Aug. 1995, pp. 127–157.

[23]Lin, J. T., and Pao, H. Y., "Wakes in Stratified Fluids," *Annual Review of Fluid Mechanics*, Vol. 11, 1979, pp. 317–338.

[24]Weast, R. C. (ed.), *CRC Handbook of Chemistry and Physics*, 65th ed., CRC Press, Boca Raton, FL, 1984, p. F-4.

[25]Liu, H.-T., "Tow Tank Simulation of Vortex Wake Dynamics," *Proceedings of FAA International Symposium on Wake Vortices*, DOT/FAA/SD-92/1.1 and DOT-VNTSC-FAA-92-7.1, Vols. 1 and 2, Paper 32, Federal Aviation Administration, U. S. Dept. of Transportation, Washington, DC, 1991, pp. 1–26.

[26]Lin, Q., Boyer, D. L., and Fernando, J. S., "The Vortex Shedding of a Streamwise-Oscillating Sphere Translating Through a Linearly Stratified Fluid," *Physics of Fluids*, Vol. 6, No. 1, 1994, pp. 239–252.

[27]Sarpkaya, T., "Trailing Vortices in Homogeneous and Density-Stratified Media," *Journal of Fluid Mechanics*, Vol. 136, 1983, pp. 65–109.

[28]Holzapfel, F., Gerz, T., and Baumann, R., "The Turbulent Decay of Trailing Vortex Pairs in Stably Stratified Environments," *Aerospace Science Technology*, Vol. 5, No. 2, 2001, pp. 95–108.

[29]Hecht, A. M., Bilanin, A. J., and Hirsh, J. E., "Turbulent Trailing Vortices in Stratified Fluids," *AIAA Journal*, Vol. 19, No. 6, 1981, pp. 691–698.

[30]Burnham, D. C., Hallock, H. N., Tombach, I. H., Brashears, M. R., and Barber, M. R., "Ground Based Measurements of a B-747 Aircraft in Various configurations," Federal Aviation Administration, Rept. FAA-RD-78-146, U. S. Dept. of Transportation, Washington, DC, Dec. 1978.

[31]Liu, H.-T., "Simultaneous Visualization of Wakes and Internal Waves Generated by Towed Cylinders in Stratified Fluids," *Journal of Flow Visualization and Image Processing*, Vol. 12, No. 2, 2005, pp. 151–174.

S. Aggarwal
Associate Editor